Al-Mustansiriyah Journal of Science

Al-Mustansiriyah Journal of Science
ISSN: 1814-635X (print) 2521-3520 (electronic)

ORIGINAL ARTICLE *OPEN ACCESS*

Estimation of the Optimum Etching Time and Etching Parameters for CR-39 Nuclear Tracks Detector by Applying Plasma and Chemical Etching Techniques

Abdulkader Makki Dahham [a], Jamoliddin Razzokov [b], Eldor Karimbaev [b], and Raghad S. Mohammed [a]

[a] *Department of Physics, College of Science, Mustansiriyah University, Baghdad, Iraq*
[b] *Institute of Fundamental and Applied Research, National Research University TIIAME, Tashkent, Uzbekistan*

CORRESPONDENCE
Raghad S. Mohammed
raghad.almaliki@uomustansiriyah.edu.iq

ARTICLE INFO
Received: Jun. 18, 2025
Revised: Aug. 13, 2025
Accepted: Aug. 26, 2025
Published: Sep. 30, 2025

ABSTRACT: ***Background:*** *CR-39 nuclear track detectors are widely used in various fields, including science, technology, astronomy, and environmental preservation, to detect and register heavy ions, neutrons, and alpha particles.* ***Objective:*** *This study aims to determine the optimal etching duration for CR-39 nuclear track detectors by comparing etching methods: The wet etching (using a water bath) and the dry etching technique (using dielectric barrier discharge (DBD) plasma).* ***Methods:*** *The traditional etching method involved immersing CR-39 detectors in a sodium hydroxide (NaOH) solution at 70 °C for varying durations. The dry etching method employed employs a non-thermal DBD plasma system to etch solid-state nuclear track detectors (SSNTDs) without the use of chemical solutions.* ***Results:*** *Photomicrographs revealed that tracks from chemical etching became clearly visible after 1 hour and developed at 5 hours. In contrast, the dry etching technique was significantly faster; tracks began to appear after just 1 minute of DBD plasma etching and were fully developed at 5 minutes. The optimum track density for DBD plasma was 20340±56 tracks/mm^2 at 3 minutes, whereas the traditional water bath method achieved an optimum track density of 5238.0±5.7 tracks/mm^2 at 2 hours. The shorter etching duration in the dry method likely facilitates the emergence of latent tracks without overlap.* ***Conclusions:*** *The bulk etch rate (V_B) for CR-39 detectors using the dry DBD plasma etching technique was faster compared to the traditional chemical etching method. This demonstrates the efficacy of the dry etching process in significantly reducing etching time required for etching SSNDs.*

KEYWORDS: *CR-39; Nuclear detectors; DBD plasma; Wet etching; Dry etching, Plasma interaction, Etching parameters*

INTRODUCTION

Radiation has consistently been an integral aspect of daily life on Earth, with humans receiving it daily. Radiation is the energy released as waves or minuscule particles from a substance, originating from either natural or human-caused events. Owing to the imperceptible characteristics of radiation, it became essential to identify suitable methods and instruments for its detection and measurement [1], [2]. There has been use of track detectors extensively in various areas of contemporary technology and science, including the detection and registration of heavy ions, rapid neutrons, radon levels, nuclear fission fragments, alpha particles, plasma physics, astronomy, radiation safety, and environmental conservation [3], [4]. The track registration techniques were initially identified by D. Young in 1958 [5]. The solid-state nuclear trace detectors (SSNTDs) function by containing ionization within a medium as it traverses through a material. An alpha particle possessing an energy of 6 MeV interacting with the cellulose nitrate produces 15×10^4 ion pairs. That equates to a mean from 3 to 4 ion pairs per nm, or 37×10^2 ion pairs per μm. The characteristics and classification of the particle, the conditions under which it is stored, the effective charge, the energy of the particle,

and the rate of full energy dissipation of radiation within the detector medium significantly influence the geometry, morphology, and dimensions of a track in solid-state nuclear trace detectors (SSNTD). Polyallyl di-glycol carbonate, commonly referred to as CR-39, serves as a prominent detector for nuclear tracks [6]–[10]. CR-39 is used in proton and radon dosimetry, the detection of charged particles in nuclear physics, and other optical applications. The primary applications of nuclear track detectors include mineralogy, dosimetry, environmental monitoring, and radiation detection [11].

The tracks were fabricated with the chemical etching (CE) technique. This mechanism accelerates chemical reactions, leading to the formation of many entities, including chemical radicals. A latent track is a compromised area created by an alpha particle, where chemical reactions are heightened when exposed to strong chemical substances, with aqueous solutions of NaOH or KOH commonly utilized in that processes. The particle's traces are discernible using the microscope lens as the chemistry solution marks the detection material. Track visualization, or "detector etching," is the term used to describe this process, while the "track effect" is the term used to describe the related phenomenon [12]–[14]. Chemical method etching is an essential technique employed in numerous surface research and technological applications [15]. Prior studies have aimed to minimize the period of etching process required for track etching, including microwave, induced traditional etching [16], ultrasonic chemical etching [14], and plasma DBD etching (dry etching).

It is known that plasma is the "fourth state" of the matter, distinct from solid, gas, and liquid [17]. Plasma is electrically neutral overall and is often characterized as a collection of excited electrons, ions, photons, atoms, radical species, and non-ionized neutral particles [18]. It may be divided into two types based on temperature: high-temperature plasma and low-temperature plasma. Dielectric barrier discharge (DBD), also known as dielectric barrier corona discharge or silent discharge, is a non-equilibrium plasma that may be created at atmospheric pressure in both open and closed configurations. DBD is defined by the release of high-energy electrons that collide with nearby gas molecules in a way that isn't flexible. This can excite or break apart the molecules to form plasma, which is made up of many different types of particles, including free radicals, excimer molecules, excited atomic and molecular entities, and particles in an excited state that have reactive chemical properties [19]–[21]. In normal chemistry, this means that some reactions need high temperatures or rare metals to work. However, these reactions can easily happen in low-temperature DBD. Within this plasma structure, charges move between two electrodes, with an insulating material, usually made of glass or clay, covering at least one of the electrodes. When they work at normal pressure, DBD plasmas are linked to cool situations [22], [23].

In this paper, the plasma etching technique, dielectric barrier discharge (DBD) plasma, as a dry etching method, will be employed to examine the efficacy of plasma interactions in recording alpha particles within a short etching duration. Subsequently, these methods will be comparison to conventional etching technique (C_E) utilizing water bath (traditional method) to the establish its for efficacy as a feasible option for the etching of nuclear trace detectors. Furthermore, various essential etching parameters influencing track formation are analyzed, including the total etching rate, track etching rate, sensitivity, and etching efficiency (V_B, V_T, V and η).

MATERIALS AND METHODS

Prepare the CR-39 SSNTDs

The plastic nuclear track detector known as Pollyallyl diglycol carbonate (PDC), which has the molecular formula [$C_{12}H_{18}O_7$], is the CR-39 nuclear detector (Columbia Resin No. 39). It was bought from Pershore Moulding Ltd. in the United Kingdom. With the density of ($132 \times 10^{-2} \frac{g}{cm^3}$), an ionization energy of 70.2 eV, and a thickness of 250 μm, CR-39 exhibits a high sensitivity to ionizing radiation [23]. As shown in Figure 1, the CR-39 detector was cut into uniform pieces (1×1) cm^2 and exposed to alpha particles with energy ($E_\alpha = 5.49 \times 10^6$ eV) and 5 μCi $\pm 5\%$ activity emitted from a radium source ^{226}Ra, which has a half-life of 1620 years, for five seconds.

Figure 1. CR-39 detector with dimensions (1 × 1) cm^2 under optical microscope

Wet Etching Technique: Traditional Method (Water Bath)

These particles possess sufficient energy to enter the CR-39 detector and interact with the polymeric materials, causing chemical bonds to break and leaves behind traces. Following the exposure process of the CR-39, etching procedure is initiated to elucidate the characteristics of the trace imprinted on the CR-39. To augment the discernibility of the tracks on the CR-39 detector, it is submerged in the alkaline solution (notably, a NaOH solution with concentration 6.25 N was employed to the etch exposure detectors in the present investigation) and maintained at a controlled heat of 70±2 °C [24]. The progression of the pits can be monitored by executing to the complete etching process at periods of 1, 2, 3, 4, and 5 hours. Tracks are formed when (OH) ions react more rapidly radiation damage compared to the surrounding polymers. Following each etching phase, the quantity of traces on the detector can be enumerated with a 40X optical microscope.

Dry Etching Technique (DBD plasma)

DBD plasma etching represents the dry etching method because it uses a non-thermal plasma system to etch SSNTDs instead of a liquid (the chemical etching solution). Dielectric barrier discharge (DBD) plasma sources have been effectively used for etching various materials, including polymers, in the last several decades. DBD plasma sources produced at atmospheric pressure were used [25]–[27]. Figure 2 illustrates the manufactured system. Two electrodes, constructed of 7.2 cm in diameter and 0.3 cm in thickness, make up the DBD plasma system. A 5 mm-thick dielectric material (Teflon) covers the electrodes. A 1 mm-thick glass plate was utilized to separate the powered and ground electrodes, and one of the poles was left to the air exposed. An AC power source with a voltage of 7000 V and a frequency of 9300 Hz was used to power the DBD reactor. As demonstrated in Figure 2, the air above the covered electrode becomes ionized and looks blue when the AC voltage supplied to the electrodes is high enough. the ionized air is plasma. The discharge gap was 2 mm, and a CR-39 detector was placed between the discharge gap and etched with plasma for 1, 2, 3, 4 and 5 minutes.

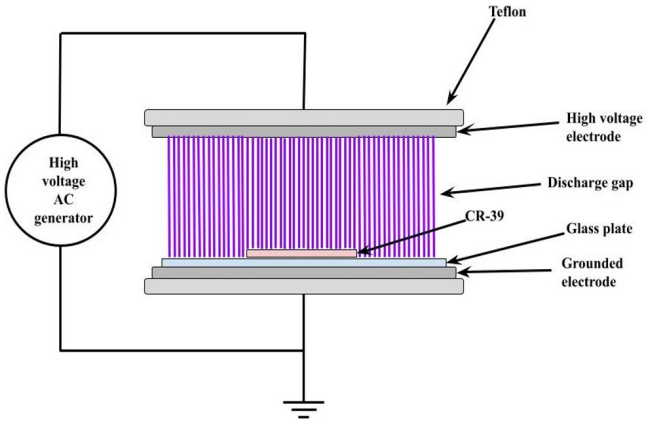

Figure 2. The manufactured dielectric barrier discharge (DBD) plasma source

Track Density and Diameter Measurement

Following each etching period, the CR-39 detectors were carefully rinsed with filtered water and allowed to air dry in order to record the track number. A 40X magnification optical microscope (N-200M, built in Korea) was used to record the total number of traces that were created on the etched CR-39 detector after each etching process. Without looking through the eyepiece of the microscope, the traces were observed through a computer linked to the digital imaging device (Digicam) (CAUTION, S/N: C1371000091). The density of the alpha particle tracks in the CR-39 detector was determined by summing total number of the particle traces (alpha particle) in five separate images for each etching period, divided by the field of vision (58×10^{-3} mm^2). To avoid including cracks and grooves in the calculated alpha particle latent path widths, great caution was exercised when measuring the tracks of these particles. Following the etching of the CR-39 detectors, the optical microscope was used to manually measure the alpha particle tracks' widths, with a measurement resolution of ± 0.5 μm. For every etching time, the diameters of thirty circular traces were recorded.

Theoretical Part

In this investigation, etching parameters are estimated to facilitate comparisons between the methods used in the etching. Table 1 illustrates the equations employed and their definitions, in addition to referencing the sources from which these equations were acquired.

Table 1. The formulas used and their definitions for calculating the etching parameters

Equation	Definition	Symbol	Reference
$V_B = \frac{D}{2t}$	The bulk etch rate (μm/h)	D: Track diameter T: Time of etching	[4], [28]
$V_T = V_B \frac{1+\left(\frac{V_D}{V_B}\right)^2}{1-\left(\frac{V_D}{V_B}\right)^2}$	The track etch rate (μm/h)	V_B: The bulk etch rate (μm/h) VD: The diameter rate of the tracks	[29], [30]
$V = \frac{V_T}{V_B}$	Sensitivity (V)		[31], [32]
$\theta_c = \sin^{-1} \frac{V_B}{V_T}$	The critical angle		[32]
$\eta = 1 - \sin\theta_c$	The etching efficiency of a detector		[4], [32]

RESULTS AND DISCUSSION

Examination of Plasma Spectra to Identify RONS Species and Quantify Plasma Jet Characteristics

Excited species generated by the DBD plasma source have been identified by optical emission spectroscopy. Spectra in the wavelength range 200–900 nm were taken at an axial distance of 1mm from the DBD plasma. Utilizing a Surwit (S3000-UV-NIR) spectrometer, we meticulously captured the emission spectra of dielectric barrier discharge (DBD) plasma, as shown in Figure 3. The detection and subsequent identification of reactive molecular species present in the plasma emissions generated by DBD plasma devices functioning under ambient pressure conditions have been performed through optical emission spectroscopy (OES) analysis. The reactive oxygen species (ROS) and reactive nitrogen species (RNS) are essential for initiating and sustaining the reaction processes. The identification of the emission bands was executed in accordance with the reference [33]. Reactive species (ROS/RNS) produced by DBD plasma may be identified by the spectral bands seen between 296 and 428 nm. By observing the peaks at 296 nm and 309 nm, we may deduce that (NO) is present, and the presence of the hydroxyl radical ($^{\bullet}OH$) is also indicated by the peaks at 309 nm. Furthermore, the wavelengths of 391, 381, 358, 358, 316, and 426 nm may suggest the existence of the low-intensity nitrogen molecular band system (N_2 second-positive system, $C_3\Pi_u$–$B_3\Pi_g$). The peak at 572 nm on the emission spectra for DBD plasma illustrated that the release also contains singlet oxygen (O). On the other hand, spectra for DBD plasma induced appear oxygen at wavelengths 693 and 871 nm.

 DOI: https://doi.org/10.23851/mjs.v36i3.1699

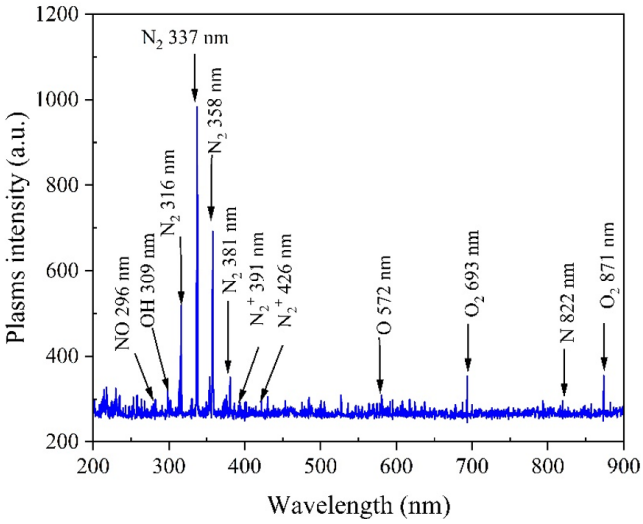

Figure 3. The optical emission spectra generated by DBD plasma discharge for the identification of reactive oxygen and nitrogen species (RONS)

In this investigation, was used spectral line broadening analysis to evaluate two parameter, maximum density, and the gas electron temperature. The formula of Doppler broadening (1) [34] was used to measure the gas temperature:

$$\Delta\lambda_{Doppler} = 7.16 \times 10^{-7}\lambda\sqrt{\frac{T}{M}} \tag{1}$$

The DBD plasma's gas temperature, as determined by the Doppler broadening analysis, is 308 K. However, the electron density may be calculated using the Stark broadening effect (2) [3], [35]:

$$\Delta\lambda_{Stark} = 2 \times 10^{-16}\mathrm{w}N_e \tag{2}$$

$\Delta\lambda_{strak}$ the full width at half maximum($\Delta\lambda_{FWHM}$) of the Stark broadening, w is the electron impact parameter, and N_e is the electron density in cm^{-3}. It is measured that there are 4.4×10^{17} cm^{-3} in the dielectric barrier discharge (DBD) plasma.

Track Development Process

Alpha particles and other forms of ionizing radiation have the potential to totally ionize the CR-39 solid-state detector's polymers, which could lead to the breaking of their chemical bonds [36]. According to Kadhim and Jebur 2018 [31]. One important feature of these detectors is their capacity to record very low activity levels, which is especially important when dealing with tissue samples [38]. Depending on the kind, energy, intensity, and angle of incidence of the radiation, the tracks can be any size, shape, or depth. Alpha particles are realized to only break through a fine layer of the CR-39 face and to have a limited material range.

The 5-MeV alpha particle range in CR-39 is 28.9 mm, according to the SRIM program [37], according to the SRIM program alpha particles with an energy of 5.49 MeV, emitted from Ra-226 decay, have an estimated projected range of approximately 30.3 μm in CR-39 detector material [37]. The energy of the entering alpha particles is typically highly correlated with the range [38]. Therefore, this becomes problematic when alpha particles have different energies. Therefore, the calculation of the density of alpha particles will be difficult because the ranges would differ. So, by trying out several etching durations, we can find the optimal one for using a new etching process. This study examined the plasma-induced etching and dry etching, using varying etching durations to find the optimal tracks. Alpha particles' different energies cause them to have different penetration ranges in detector materials.

The etching time required for the latent alpha particle tracks of lower energy particles to be visible in the CR-39 detector is longer. Figures 3a–e shows the photomicrographs of the CR-39 detector obtained at 1, 2, 3, 4, and 5 hours in order to determine the optimal etching time for the CR-39

nuclear trace detector using traditional chemical etching by a water bath approach (CE). Because the detectors were irradiated to alpha particles without a radiation guide, both circular and oval tracks were produced, as shown in the Figure 4.

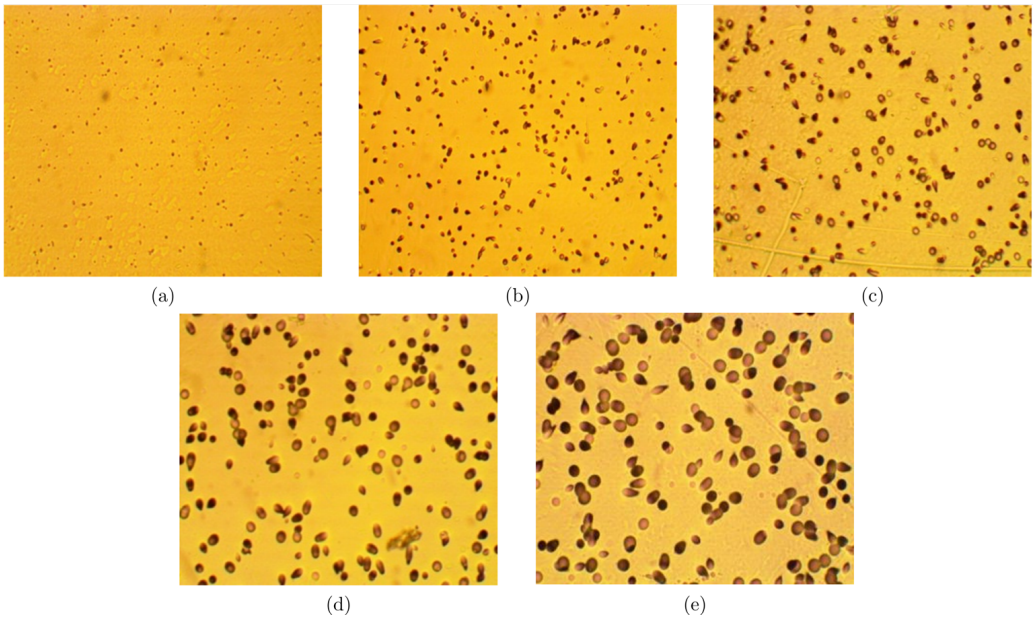

Figure 4. Formation of latent alpha trace in CR-39 detectors using chemical etching for different etching durations in a water bath: (a) At 1 hour; (b) At 2 hours; (c) At 3 hours; (d) At 4 hours; (e) At 5 hours of engraving duration

Latent tracks or hidden tracks denote damage zones formed by ionizing particles in a material. Upon exposure to a chemically reactive solution, these zones undergo accelerated etching. Aqueous sodium hydroxide (NaOH) is the most widely utilized etchant in such processes. The surface of the detector material is generally etched by the chemical solution, but the damaged region etching occurs more quickly. This is one way a particle's "track" can be seen under an optical microscope. It's known as the "track effect," and the technique is known as "track visualization" or "detector etching" [12], [23], [39].

Figure 4 shows that with an increase in etching duration, the quantity of tracks not only increases but also becomes clearer. Figure 4a shows that hidden traces of alpha particles start to show up after one hour of etching. Both the total number of traces and their visibility grow with increasing etching time. Results recorded in Table 2, we discovered that the CR-39 detectors produced 283.0±9.3 tracks in one hour and 308.0±5.7 tracks in two hours. The intensified interaction between the aggressive solution and the compromised regions resulting from the impact of the alpha (^4He) particles on the detector material constitutes the origin of the escalation in the quantity of tracks. Furthermore, given that low-energy alpha particle tracks exert a diminished influence on the detector material and require an extended etching duration, the observed phenomenon of increase in the total number of traces concomitant with prolonged etching duration may be attributable to the existence of these tracks. On the other hand, as the etching duration increased, we observed fewer traces, as illustrated in Figures 4c-e. It is hypothesized that the overlap of tracks is the reason why the total number of traces dropped from 205.0±13.1 tracks at an etching duration of 3 hours to 172.1±11.2 traces at the final period of the etching process, or at an etching duration of five hours.

Equation 3 is applied to quantify density of the traces after each etching duration step, enabling the observation of track growth and the assessment of the optimal etching duration [40], [41].

$$\rho = \frac{N_{ave}}{A} \tag{3}$$

where ρ: Track density in Track/mm^2, Nave: Average total number of traces, and A: Field of the view area ($588 \times 10^{-4}\ mm^2$).

The findings derived from the chemical traditional etching procedure utilizing a water bath, as delineated in the Table 1, indicate that density of the alpha traces attained its apex at an etching

duration of two hours (5238±6.0 tracks). As the etching time was prolonged, the track density exhibited a decline, diminishing from 3487±13.10 tracks at 3 hours to 2925±11.10 tracks at 5 hours. The quantification of track density is contingent upon the aggregate number of tracks formed on the CR-39 detector. Figure 5 illustrates that a decline in track density is concomitant with an increase in track diameter as etching duration is extended. This occurrence is attributed to the adjacency overlapping of the traces, which engenders an augmentation in track diameter. Continuous etching process may lead to a secondary overlap of the traces. The merging of these processes leads to a reduction in the total traces number and, therefore a drop in trace density, resulting in an augmented growth of track diameters. Figures 6 and 7 illustrate the histogram dispersions related to the lengths and diameters of the alpha particle traces, respectively, derived from 30 tracks that were randomly selected, encompassing both circular and oval forms. These tracks were etched over a range of durations during the chemical etching process conducted in a water bath regulated at a heat of 70±2 °C.

Table 2. Trace density and diameter measurements in CR-39 detectors utilizing a water bath chemical etching technique at varying etching times

Etching Time (Hour)	**No. tracks (mean±S. D)**	**Track density (mean±S. D) (Track/mm^2)**	**D (μm) (mean±S. D)**
1	283.0±22.5	4813.0 ±22.50	3.10±0.62
2	308.0±5.7	5238.0±6.0	7.6.00±0.77
3	205.0±13.1	3487.0±13.10	8.80±1.17
4	181.0±10.1	3078.0±10.10	11.40±1.43
5	172.0±11.1	2925.0±11.10	16.50±1.49

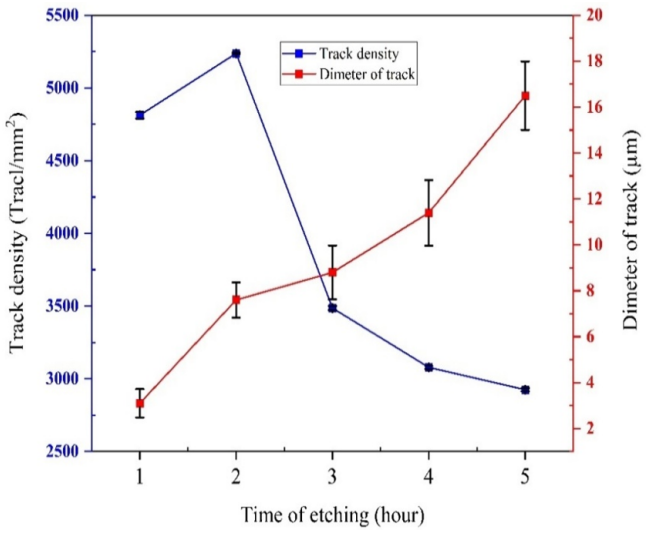

Figure 5. Track density and diameter development using chemical etching at different etching periods

We will employ the DBD plasma for the dry etching process at atmospheric pressure and compare the outcomes with the etching techniques previously employed by using sodium hydroxide solution with water bath.

Figures 8a-e illustrate results of dry etching by DBD plasma for varying etching times (1, 2, 3, 4, and 5 minutes). During the first minute of etching, the tracks are clearly visible, this is due to the direct plasma discharge onto the nuclear detector CR39, which occurs without the presence of an intermediate chemically aggressive solution such as NaOH. Figure 8a shows that the hidden traces of the particles in detector were revealed by a 1-minute etching time, yielding 421 tracks. Figures 8d-c show that the total number of traces increases and becomes visible as the etching time increases.

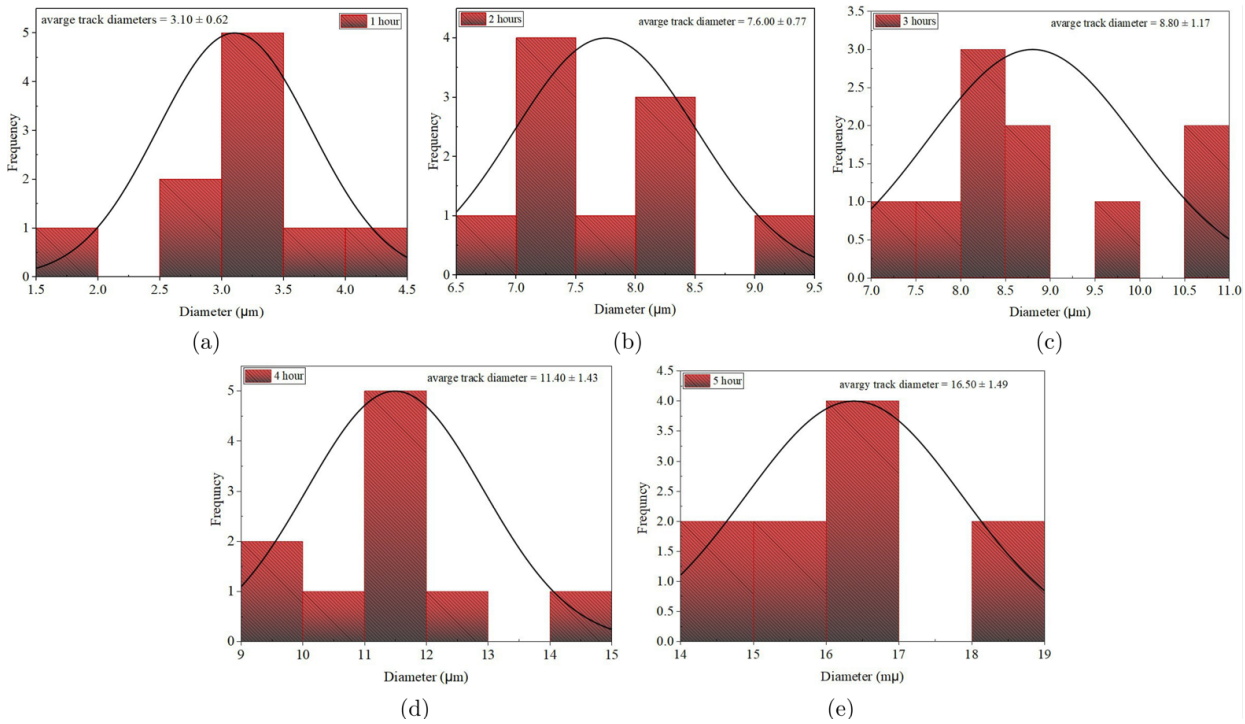

Figure 6. Diameters analysis of thirty alpha particles tracks in CR-39 detectors chemically etched in 6.25 N NaOH at 70±2 °C and varying etching times: (a) After 1 hour; (b) After 2 hours; (c) After 3 hours; (d) After 4 hours; (e) After 5 hours

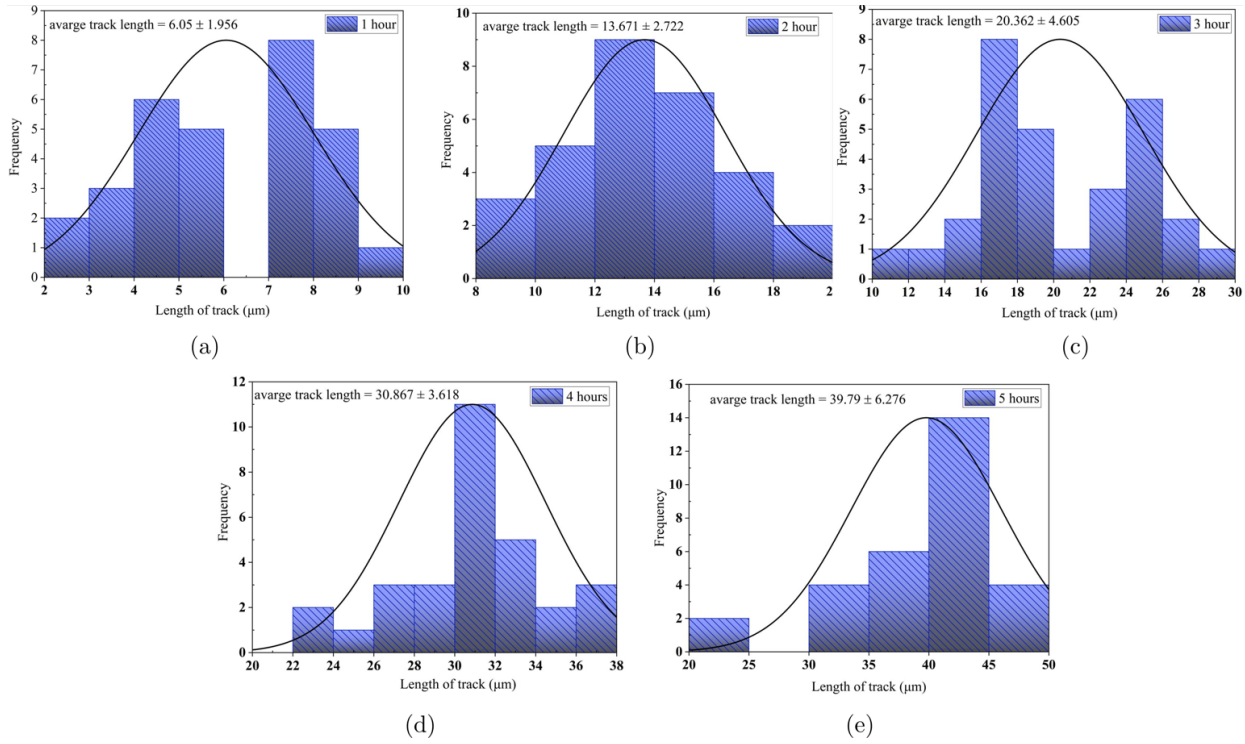

Figure 7. Lengths analysis of thirty alpha particles tracks in CR-39 detectors chemically etched in 6.25 N NaOH at 70±2 °C and varying etching times: (a) After 1 hour; (b) After 2 hours; (c) After 3 hours; (d) After 4 hours; (e) After 5 hours

Several tracks grow with etching time, reaching a maximum of 1196 tracks at 3 minutes. Due to nearby nuclear tracks overlapping, the number of tracks decreases to 454 tracks Figure 8e, but the track diameter keeps growing with increasing etching time, 4.02 μm, except for the second etching time, where the diameter will decrease by 0.12 μm because of the appearance of doubleted tracks number from the first etching time.

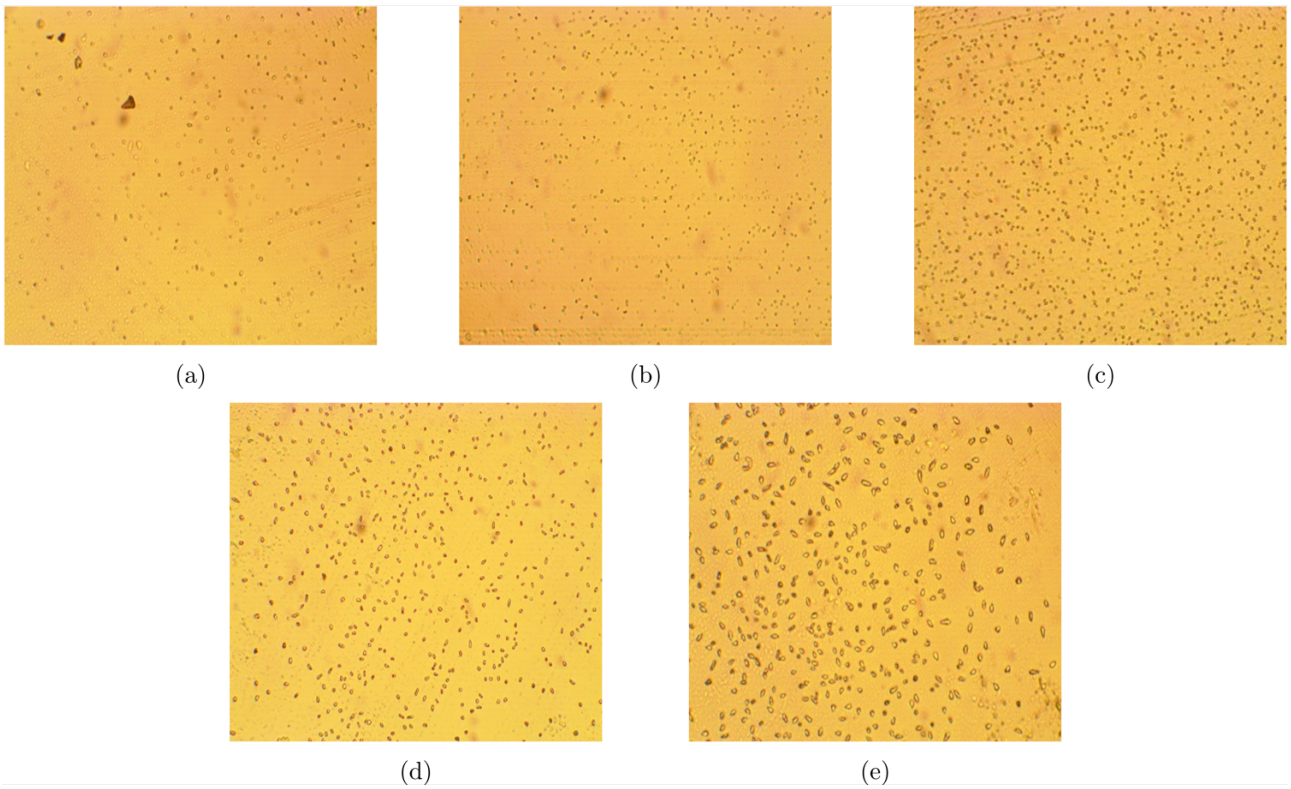

Figure 8. Formation of latent alpha tracks in CR-39 detectors using DBD plasma for etching at different durations: (a) at 1 min; (b): at 2 min; (c): at 3 min; (d) at 4 min; (e) at 5 min

Dry plasma etching is a physical procedure that is different from traditional etching technique (using a water bath). Only the deformed regions created through the alpha particles' interaction with the detector material are affected by the plasma beam when it meets its surface. Their depth or surface area increases because of the beam breaking bonds in these regions. When looking at the detectors under a microscope, this increase makes the tracks more visible. Table 3 presents the results obtained from the dry etching process.

Table 3. Assessment of track density and diameters in CR-39 detectors exposed to DBD plasma etching over various times

Etching Time (minute)	**Tracks No. (mean±S. D)**	**Track density (Track/mm^2) (mean±S. D)**	**Diameter (μm) (mean±S. D)**
1	421±51	7159±51	1.72±1.11
2	801±57	13622±57	1.60±0.85
3	1196±56	20340±56	2.08±1.14
4	595±10	10119±10	2.28±0.99
5	454±51	7721±51	4.02±1.72

Figure 9 shows the improvement on traces density consistent with increasing etching duration the trace density of 20340 Track/mm^2 at 3 minutes, after which the tracks begin to overlap and reach 7721±51 Track/mm^2 at 5 minutes of etching time. We observed a continuous expansion in

the diameter of tracks with increasing etching time. Figures 10 and 11 illustrate the histogram distributions pertaining to the lengths and diameters of alpha particle traces, respectively, derived from 30 tracks that have been randomly selected, for both circular and elliptical forms, which were etched over a range of durations during the DBD plasma etching process conducted in maintained at heat of 32±2 °C.

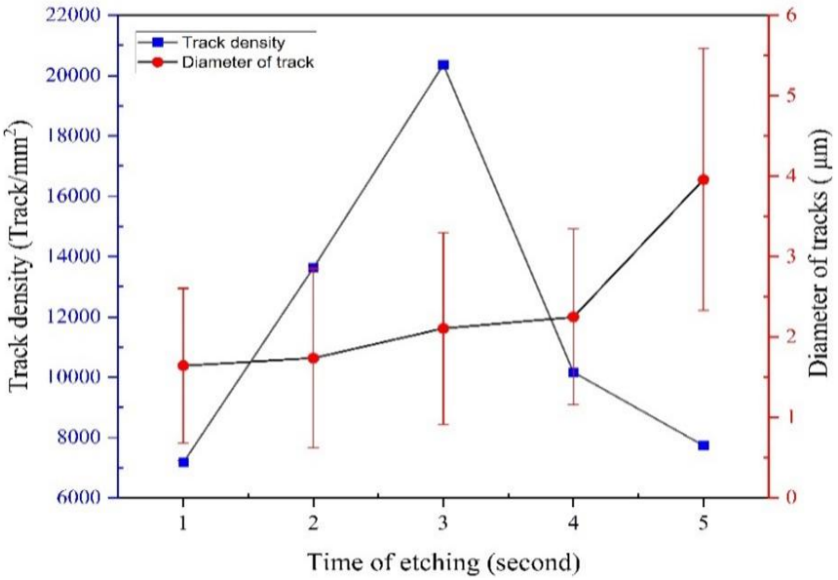

Figure 9. Track density and diameter development using DBD plasma for etching at different etching periods

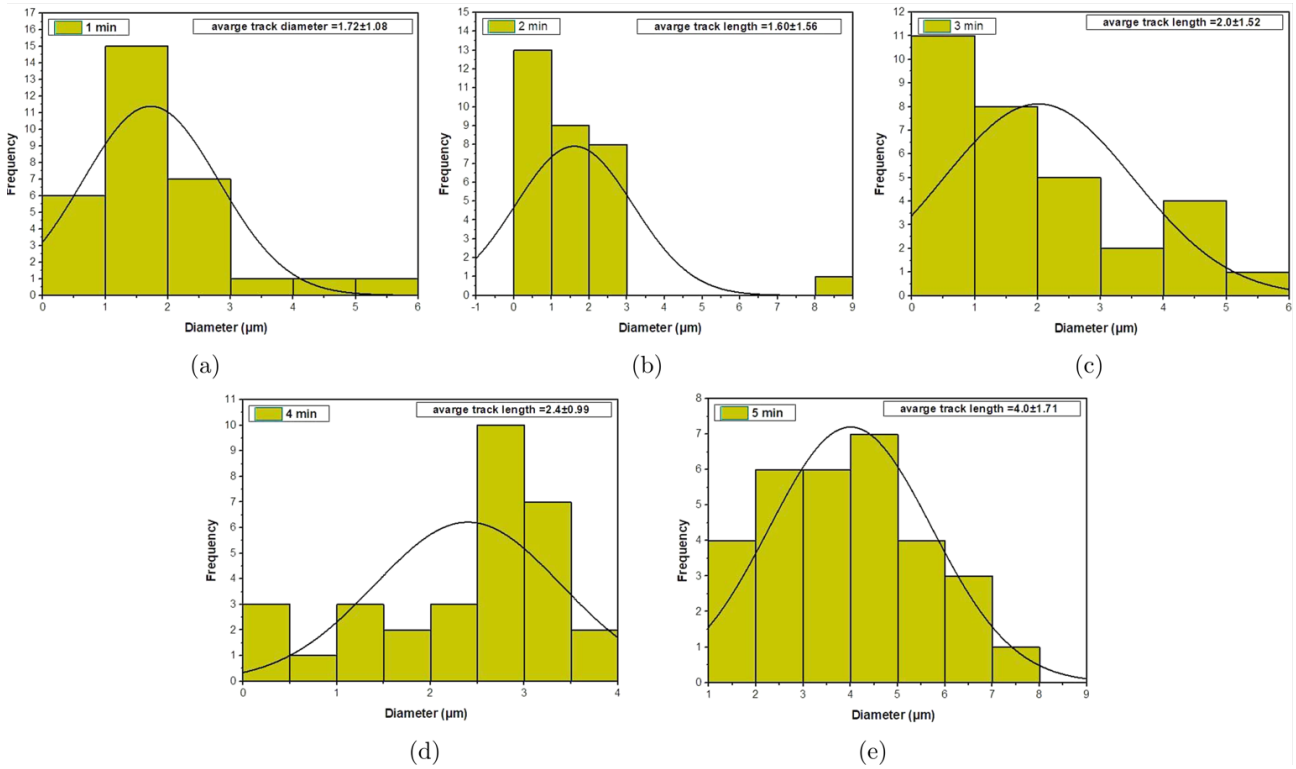

Figure 10. Diameters analysis of thirty alpha particles traces in CR-39 detectors that etched by DBD plasma at 32±2 °C and varying etching times: (a) After 1 min; (b) After 2 min; (c) After 3 min; (d) After 4 min; (e) After 5 min

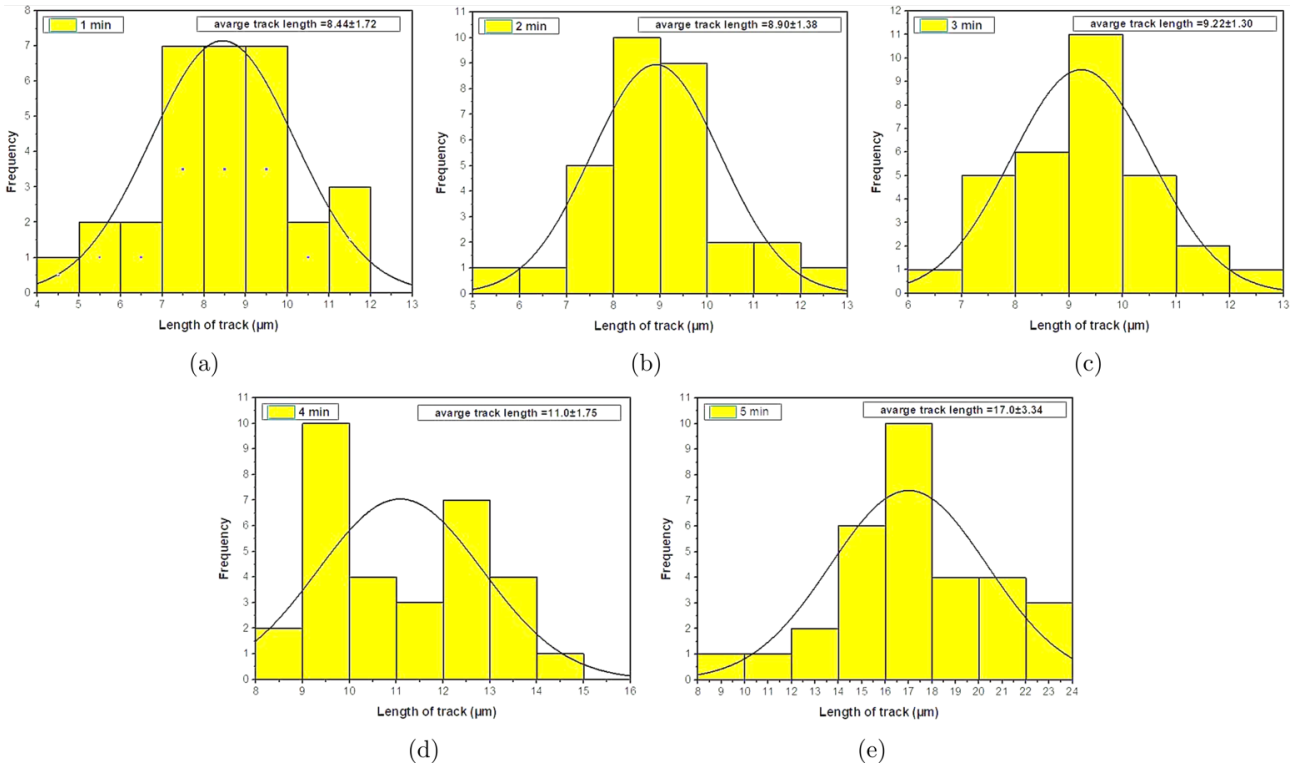

Figure 11. Lengths Diameters analysis of thirty alpha particles traces in CR-39 detectors that etched by DBD plasma at 32±2 °C and varying etching times: (a) After 1 min; (b) After 2 min; (c) After 3 min; (d) After 4 min; (e) After 5 min

Etching Parameters

Table 1 establishes the employed equations and their meanings, together with citations of the sources from which these equations were derived.

Through the utilization of the equations presented in Table 1, the etching parameters (V_B, V_T, V, θ, and η) pertinent to the CR-39 nuclear track detector were computed. The bulk etch rate (V_B), which indicates the rate at which the bulk material dissolves in solution and makes it easier for tracks to develop, is a crucial component in the etching process. In accordance with the optimal track density, V_B was ascertained to be $2 \times 10^{-6} \frac{m}{h}$ under the specified etching conditions (NaOH with concentration 6.25 N, 70±2 °C, 120 min), a value that is inferior to that reported by researchers employing nearly analogous etching environment (NaOH with concentration 6.25 N, 85 °C, 180 min) [42], [43]. This variation might be caused by differences in the chemical solution's heating temperature and the etching process's time. In contrast, during the optimal etching period, the average etching rate for DBD plasma etching was approximately 20.8 μm/h. These findings are delineated in Table 4, which summarizes the etching methodologies employed (water bath and DBD plasma).

The track etching rate (V_T) was determined by the rate of the track diameter and the bulk etch rate (V_B). The rate of change in the track diameter was found by finding the slope of the graph that showed the relationship between the etching time and the track diameter. As shown in Figure 12, this examination was done separately for both chemical etching in a water bath and DBD plasma etching. Figure 12 indicates that under the specified etching conditions for both methodologies, an increase in the removed layer corresponded with a subsequent increase in track diameter.

The detector's sensitivity is another critical factor in the etching process being examined. n etched track detector's sensitivity (V) to alpha particles depends on several factors, including the charge, energy, and trajectory of the incoming ions and the detector's basic material properties [44]. The sensitivity (V) of nuclear detector CR-39 was ascertained through the assessment of the track diameter rate (V_D) and the bulk etch rate (V_B).

Table 4. CR-39 detector etching factors at various etching times for two distinct methods (chemical etching and DBD plasma)

Time of etching (hour)	V_B (μm/h)	V_T (μm/h)	V	θ_c	η %
chemical etching					
1	1.55	2.60	1.68	57	46
2	2	4.24	2.23	44	57
3	1.47	2.33	1.59	59	43
4	1.43	2.20	1.55	61	42
5	1.65	2.98	1.81	53	49
DBD plasma etching					
0.016	53.75	110.5	2.0	46	54
0.033	24.25	93.5	3.8	25	74
0.05	20.81	52.6	2.5	38	62
0.066	17.29	31.9	1.8	51	50
0.083	24.23	93.1	3.8	25	74

The sensitivity of the detector exhibits variability in relation to the duration of the etching process, as delineated in Table 4. The findings demonstrated that, at the identified optimal etching duration, the sensitivity of the detector was markedly superior for DBD plasma etching in comparison to chemical etching, as depicted in Table 5. A crucial metric for CR-39 detectors is the etching efficiency. The ratio of tracks registered, articulated as a fraction of the particles impacting the detector surface, is termed the etching efficiency of the detector [45]. The findings demonstrated that, at the optimal etch duration found, the etching effectiveness for DBD plasma etching (62%) surpassed that of chemical etching (52%), as illustrated in Table 5. Measurements of the critical angle (θ_c) were utilized to determine the etching effectiveness of the CR-39 nuclear detector. The results indicate that the dry etching technique (DBD Plasma) is an effective method for etching solid-state nuclear track detectors (SSNTDs).

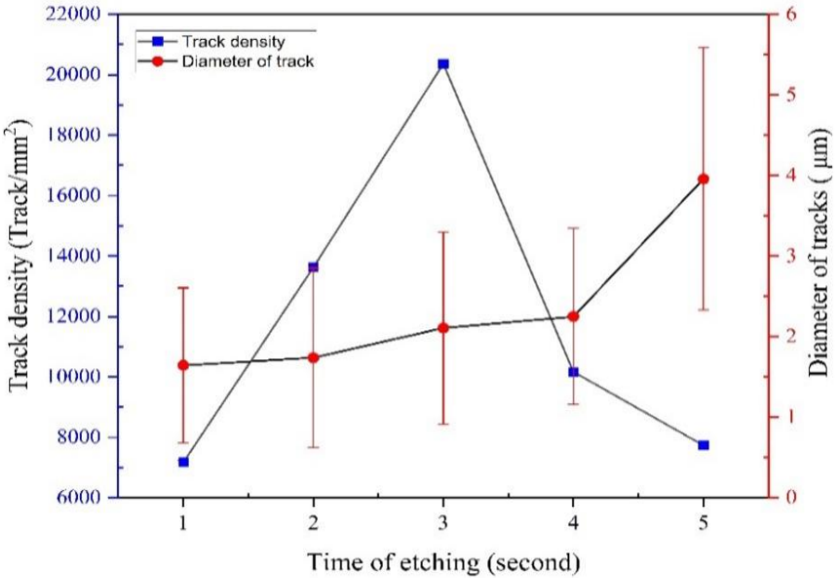

Figure 12. The tracks' diameter as a function of etching time using both the DBD plasma etching technique and the conventional water bath etching approach

Table 5. Etching parameters of CR-39 detector at optimum etching times for two techniques (chemical etching and DBD plasma)

Etching technique	**Optimum etching time (min)**	**Optimum Track density (Track/mm^2)**	V_B ($\frac{\mu m}{h}$)	V_T ($\frac{\mu m}{h}$)	V	θ_c	η%
Chemical etching	120	308.0±5.7	1.9	4.24	2.23	44	54
DBD plasma (dry etching)	3	20340±56	20.8	52.6	2.5	38	62

CONCLUSION

The SSNTD CR-39 detector's etching parameters were determined and compared for two different etching techniques: chemical etching (wet etching) and DBD plasma etching (dry etching). Experimental measurements of the track diameters and densities from the three etching techniques at various etching times were conducted. The etching parameters (V_B, V_T, V, and η) for the CR-39 track detector were computed based on the experimental findings. Compared to DBD plasma (dry etching) and traditional chemical etching (CE), DBD plasma was found to be a faster and more promising technology. Unlike chemical etching with a water bath, the etching process may begin immediately rather of waiting for the required temperature to be reached and maintained. The process of track development generally requires only a same minute, in contrast to the numerous hours necessary for the etching traditional technique. Additionally, the elevated $\frac{V_T}{V_B}$ ratio that results from preferential etching along the track improves the track revelation process. This improvement includes enhanced clarity, uniform etching, and increased detecting efficacy, all of which are beneficial. The results conclude that the optimum etching time when using the traditional method (chemical etching) was at an etching time of two hours, 5238 track/mm^2, as for the dry etching technique using DBD plasma, the optimum etching time was at 3 minutes, 20340 track/mm^2. Plasma etching is far faster than chemical etching; it takes only five minutes instead of 1 hour or more. The following is a rundown of the steps used to make a plasma device for etching, which will allow you to compare the results with chemical etching.

SUPPLEMENTARY MATERIAL

None.

AUTHOR CONTRIBUTIONS

Abdulkader Makki Dahham: Formal analysis, Software, and writing—original draft. Raghad S. Mohammed: Conceptualization, Methodology, Investigation, Supervision, and Writing—review & editing. Jamoliddin Razzokovb: Investigation, Review and editing. Eldor Karimbaevb: Review and editing. Nada Farhan Kadhima: Investigation and Supervision.

FUNDING

This research received no external funding.

DATA AVAILABILITY STATEMENT

Data are available from the authors upon reasonable request.

ACKNOWLEDGMENTS

The authors sincerely acknowledge the valuable support and assistance provided by the department of microbiology, college of science, mustansiriyah University. Their contributions were instrumental in facilitating the completion of this research.

CONFLICTS OF INTEREST

The author Raghad S. Mohammed, declares a conflict of interest as an editorial board member of Al-Mustansiriyah journal of science. To ensure a fair review process, she had no role in handling or decision-making for this submission. The manuscript was handled independently by Mostafa Yuness Abdelfatah Mostafa, section editor.

REFERENCES

[1] N. Frane and A. Bitterman, *Radiation Safety and Protection*. StatPearls Publishing, Treasure Island (FL), 2025. [Online]. Available: http://europepmc.org/books/NBK557499.

[2] A. Khan, S. Al Qahtani, W. AL- Maqbool, T. I. Al-Naggar, M. Alhamami, and A. M. Abdalla, "Efficient and fast detection of alpha particles using CR-39 detector," *Radiation Physics and Chemistry*, vol. 213, p. 111 237, Dec. 2023, doi: 10.1016/j.radphyschem.2023.111237.

[3] K. A. Aadim, K. A. Ahmed, and R. S. Mohammed, "Diagnostic analysis of Cu and CuZn plasma produced by Nd: YAG nanosecond laser at 1064 nm," *AIP Conference Proceedings*, vol. 2402, Art no. 080018, 2021, doi: 10.1063/5.0068739.

[4] N. Dwaikat, "Charge particle spectroscopy: A solid-state nuclear track detector (SSNTD)-based spectrometer," *Arabian Journal for Science and Engineering*, vol. 49, no. 1, pp. 1237–1243, 2023, doi: 10.1007/s13369-023-08284-9.

[5] M. El-Deep, F. Abdel-Wahab, N. El-Faramawy, and H. Abdelmaksoud, "Influence of irradiation of CR-39 with α-particles on the optical dispersion parameters: Role of chemical etching to develop nuclear tracks," *Radiation Physics and Chemistry*, vol. 193, Art no. 109965, Apr. 2022, doi: 10.1016/j.radphyschem.2022.109965.

[6] M. Shoeib, M. A. El-Apasery, D. A. Ahmed, and A. Abd-Elraheem, "Determination of Radium concentration and Radon Exhalation Rates Using CR-39 Detector for Different Geopolymer Cement Samples Containing Industrial Wastes," *Radiation Physics and Chemistry*, vol. 222, Art no. 111790, Sep. 2024, doi: 10.1016/j.radphyschem.2024.111790.

[7] M. Adelikhah, A. Shahrokhi, M. Imani, S. Chalupnik, and T. Kovács, "Radiological assessment of indoor radon and thoron concentrations and indoor radon map of dwellings in Mashhad, Iran," *International Journal of Environmental Research and Public Health*, vol. 18, no. 1, Art no. 141, 2020, doi: 10.3390/ijerph18010141.

[8] N. F. Kadhim, A. A. Ridha, M. D. Salim, M. Hanfi, and M. Y. Mostafa, "Development of alpha tracks measurement with thermal oven as an etching technique for SSNTDs," *Materials Today: Proceedings*, vol. 44, pp. 2903–2908, 2021, doi: 10.1016/j.matpr.2020.12.232.

[9] R. S. Mohammed, R. S. Ahmed, and R. O. Abdaljalil, "Estimation of radon activity concentration in Abu Al-Khaseb and Ad Dayer soil in southern Iraq using CR-39 detector," *Environmental Earth Sciences*, vol. 80, no. 5, Art no. 198, 2021, doi: 10.1007/s12665-021-09512-x.

[10] N. Alene Assefa, "Analysis of ^{226}Ra content and ^{222}Rn exhalation rates in soil samples from Wukro, Tigray, using SSNTDs," *F1000Research*, vol. 14, no. 289, Art no. 289, 2025, doi: 10.12688/f1000research.160449.1.

[11] K. C. C. Pires, M. Assunção, M. A. Rana, S. Guedes, R. Künzel, and N. M. Trindade, "Etching and optical properties of 1–2 MeV alpha particles irradiated CR-39 radiation detectors," *Nuclear Instruments and Methods in Physics Research Section A: Accelerators, Spectrometers, Detectors and Associated Equipment*, vol. 1041, Art no. 167370, Oct. 2022, doi: 10.1016/j.nima.2022.167370.

[12] D. Nikezic and K. Yu, "Formation and growth of tracks in nuclear track materials," *Materials Science and Engineering: R: Reports*, vol. 46, no. 3–5, pp. 51–123, 2004, doi: 10.1016/j.mser.2004.07.003.

[13] M. A. Rana, "CR-39 nuclear track detector: An experimental guide," *Nuclear Instruments and Methods in Physics Research Section A: Accelerators, Spectrometers, Detectors and Associated Equipment*, vol. 910, pp. 121–126, Dec. 2018, doi: 10.1016/j.nima.2018.08.077.

[14] N. Stevanovic, V. Markovic, M. Milosevic, A. Djurdjevic, J. Stajic, B. Milenkovic, and D. Nikezic, "Correlations between track parameters in a solid-state nuclear track detector and its diffraction pattern," *Radiation Physics and Chemistry*, vol. 193, Art no. 109986, Apr. 2022, doi: 10.1016/j.radphyschem.2022.109986.

[15] P. Henderson, "(R. L.) Fleischer, (P. B.) Price, and (R. M.) Walker. Nuclear Tracks in Solids: Principles and Applications. Berkeley and London (Univ. California Press), 1975. xxii+605 pp., 205 figs., I pl. Price," *Mineralogical Magazine*, vol. 42, no. 322, pp. 306–307, 1978, doi: 10.1180/minmag.1978.042.322.40.

[16] A. Pandey, P. Kalsi, and R. Iyer, "Effects of high intensity ultrasound in chemical etching of particle tracks in solid state nuclear track detectors," *Nuclear Instruments and Methods in Physics Research Section B: Beam Interactions with Materials and Atoms*, vol. 134, no. 3–4, pp. 393–399, 1998, doi: 10.1016/s0168-583x(97)00735-0.

[17] N. M. Brown and Z. H. Liu, "The etching of natural alpha-recoil tracks in mica with an argon RF-plasma discharge and their imaging via atomic force microscopy," *Applied Surface Science*, vol. 93, no. 2, pp. 89–100, 1996, doi: 10.1016/0169-4332(95)00329-0.

[18] Y. Todorova, E. Benova, P. Marinova, I. Yotinov, T. Bogdanov, and Y. Topalova, "Non-Thermal atmospheric plasma for microbial decontamination and removal of hazardous chemicals: An overview in the circular economy context with data for test applications of microwave plasma torch," *Processes*, vol. 10, no. 3, Art no. 554, 2022, doi: 10.3390/pr10030554.

[19] F. do Nascimento, S. Moshkalev, and M. Machida, "Changes in properties of dielectric barrier discharge plasma jets for different gases and for insulating and conducting transfer plates," *Brazilian Journal of Physics*, vol. 47, no. 3, pp. 278–287, 2017, doi: 10.1007/s13538-017-0492-1.

[20] J. He, X. Wen, L. Wu, H. Chen, J. Hu, and X. Hou, "Dielectric barrier discharge plasma for nanomaterials: Fabrication, modification and analytical applications," *TrAC Trends in Analytical Chemistry*, vol. 156, Art no. 116715, Nov. 2022, doi: 10.1016/j.trac.2022.116715.

[21] R. S. Mohammed and M. F. Al -Marjani, "DBD plasma as a practical approach to sterilization of dental instruments," *Physica Scripta*, vol. 99, no. 4, Art no. 045601, 2024, doi: 10.1088/1402-4896/ad2e5a.

[22] D. Astanei, R. Burlica, D.-E. Cretu, M. Olariu, I. Stoica, and O. Beniuga, "Treatment of polymeric films used for printed electronic circuits using ambient air DBD non-thermal plasma," *Materials*, vol. 15, no. 5, Art no. 1919, 2022, doi: 10.3390/ma15051919.

[23] C. Sabbarese, F. Ambrosino, and V. Roca, "Analysis by scanner of tracks produced by radon alpha particles in CR-39 detectors," *Radiation Protection Dosimetry*, vol. 191, no. 2, pp. 154–159, 2020, doi: 10.1093/rpd/ncaa140.

[24] M. D. Salim, A. A. Ridha, N. F. Kadhim, and A. E. Taher, "Effects of changing the exposure time of CR-39 detector to alpha particles on etching conditions," *Journal of Radiation and Nuclear Applications*, vol. 5, no. 2, pp. 119–125, 2020, doi: 10.18576/jrna/050206.

[25] P. Cools, L. Astoreca, P. S. Esbah Tabaei, M. Thukkaram, H. De Smet, R. Morent, and N. De Geyter, "Surface treatment of polymers by plasma," *Surface Modification of Polymers*, pp. 31–65, Nov. 2019, doi: 10.1002/9783527819249.ch2.

[26] P. Dimitrakellis, F. Faubert, M. Wartel, E. Gogolides, and S. Pellerin, "Plasma surface modification of epoxy polymer in air DBD and gliding arc," *Processes*, vol. 10, no. 1, Art no. 104, 2022, doi: 10.3390/pr10010104.

[27] Reema, R. R. Khanikar, H. Bailung, and K. Sankaranarayanan, "Review of the cold atmospheric plasma technology application in food, disinfection, and textiles: A way forward for achieving circular economy," *Frontiers in Physics*, vol. 10, Art no. 942952, Sep. 2022, doi: 10.3389/fphy.2022.942952.

[28] S. A. Durrani and R. K. Bull, *Solid state nuclear track detection: Principles, methods and applications*. Elsevier BV, 1987. doi: 10.1016/C2013-0-02771-5.

[29] S. Tripathy, R. Kolekar, C. Sunil, P. Sarkar, K. Dwivedi, and D. Sharma, "Microwave-induced chemical etching (MCE): A fast etching technique for the solid polymeric track detectors (SPTD)," *Nuclear Instruments and Methods in Physics Research Section A: Accelerators, Spectrometers, Detectors and Associated Equipment*, vol. 612, no. 2, pp. 421–426, 2010, doi: 10.1016/j.nima.2009.10.096.

[30] S. A. Durrani and R. Ilic, *Radon measurements by etched track detectors: Applications in radiation protection, earth sciences and the environment*. World Scientific, Jun. 1997, doi: 10.1142/3106.

[31] N. F. Kadhim and L. A. Jebur, "Investigation of the favorable etching time of CN-85 nuclear track detector," *Applied Radiation and Isotopes*, vol. 135, pp. 28–32, May 2018, doi: 10.1016/j.apra diso.2018.01.004.

[32] M. D. Salim, A. A. Marzaali, H. Khalaf, and M. Mostafa, "Comparison between etching techniques for solid-state nuclear track detector (CN-85) to develop alpha tracks," *Radiation Physics and Chemistry*, vol. 213, Art no. 111224, Dec. 2023, doi: 10.1016/j.radphyschem.2023.111224.

[33] V. Barone, S. Alessandrini, M. Biczysko, J. R. Cheeseman, D. C. Clary, A. B. McCoy, R. J. DiRisio, F. Neese, M. Melosso, and C. Puzzarini, "Computational molecular spectroscopy," *Nature Reviews Methods Primers*, vol. 1, no. 1, Art no. 38, 2021, doi: 10.1038/s43586-021-00034-1.

[34] A. Ionascut-Nedelcescu, C. Carlone, U. Kogelschatz, D. V. Gravelle, and M. I. Boulos, "Calculation of the gas temperature in a throughflow atmospheric pressure dielectric barrier discharge torch by spectral line shape analysis," *Journal of Applied Physics*, vol. 103, no. 6, Art no. 063305, 2008, doi: 10.1063/1.2891419.

[35] K. A. Ahmed, K. A. Aadim, and R. S. Mohammed, "Investigation the energy influence and excitation wavelength on spectral characteristics of laser induced MgZn plasma," *AIP Conference Proceedings*, vol. 2402, Art no. 080004, 2021, doi: 10.1063/5.0065374.

[36] R. S. Ahmed and R. S. Mohammed, "Assessment of uranium concentration in blood of Iraqi females diagnosed with breast cancer," *Radiation and Environmental Biophysics*, vol. 60, no. 1, pp. 193–201, 2020, doi: 10.1007/s00411-020-00881-8.

[37] J. F. Ziegler, M. Ziegler, and J. Biersack, "SRIM – The stopping and range of ions in matter (2010)," *Nuclear Instruments and Methods in Physics Research Section B: Beam Interactions with Materials and Atoms*, vol. 268, no. 11–12, pp. 1818–1823, 2010, doi: 10.1016/j.nimb.2010.02.091.

[38] A. M. Abdalla, T. I. Al-Naggar, R. H. Alhandhal, and H. B. Albargi, "Registration of alpha particles using CR-39 nuclear detector," *Nuclear Instruments and Methods in Physics Research Section A: Accelerators, Spectrometers, Detectors and Associated Equipment*, vol. 1042, Art no. 167419, Nov. 2022, doi: 10.1016/j.nima.2022.167419.

[39] H. Alameri, Y. Abou-Ali, M. Obeid, and R. Shweikani, "Estimation of alpha exposure on CR-39 detector using a UV-VIS spectrophotometer," *Applied Radiation and Isotopes*, vol. 209, Art no. 111331, Jul. 2024, doi: 10.1016/j.apradiso.2024.111331.

[40] A. M. Dahham and N. F. Kadhim, "Determination of the energy of the incident alpha particle by the diameter of the track registered in CR-39 detector," *AIP Conference Proceedings*, vol. 2386, Art no. 080041, 2022, doi: 10.1063/5.0067120.

[41] K. N. Yu, F. M. F. Ng, J. P. Y. Ho, C. W. Y. Yip, and D. Nikezic, "Measurement of parameters of tracks in CR-39 detector from replicas," *Radiation Protection Dosimetry*, vol. 111, no. 1, pp. 93–96, 2004, doi: 10.1093/rpd/nch367.

[42] A. A. Azooz and M. A. Al-Jubbori, "Interrelated temperature dependence of bulk etch rate and track length saturation time in CR-39 detector," *Nuclear Instruments and Methods in Physics Research Section B: Beam Interactions with Materials and Atoms*, vol. 316, pp. 171–175, Dec. 2013, doi: 10.1016/j.nimb.2013.09.001.

[43] G. Sahoo, S. Tripathy, and T. Bandyopadhyay, "Optimization of microwave-induced chemical etching for rapid development of neutron-induced recoil tracks in CR-39 detectors," *Nuclear Instruments and Methods in Physics Research Section A: Accelerators, Spectrometers, Detectors and Associated Equipment*, vol. 739, pp. 83–88, Mar. 2014, doi: 10.1016/j.nima.2013.12.037.

[44] Y. Rammah, O. Ashraf, A. Abdalla, M. Eisa, A. Ashry, and T. Tsuruta, "Fast detection of alpha particles in DAM–ADC nuclear track detectors," *Radiation Physics and Chemistry*, vol. 107, pp. 183–188, Feb. 2015, doi: 10.1016/j.radphyschem.2014.10.013.

[45] P. Rumbach, D. M. Bartels, R. M. Sankaran, and D. B. Go, "The effect of air on solvated electron chemistry at a plasma/liquid interface," *Journal of Physics D: Applied Physics*, vol. 48, no. 42, Art no. 424001, 2015, doi: 10.1088/0022-3727/48/42/424001.